



# Absorptivity of silicon solar cells obtained from luminescence

T. Trupke, E. Daub, P. Würfel\*

*Institut für Angewandte Physik, Universität Karlsruhe, D-76128 Karlsruhe, Germany*

Received 14 April 1997

---

## Abstract

Electroluminescence spectra were measured on textured and non-textured silicon solar cells at room temperature. From these spectra the absorptivity for band-to-band transitions  $A_{\text{BB}}(h\omega)$  of these solar cells could be extracted by application of the generalized Planck's law for the emission of luminescence via direct or indirect transitions.

Our method is an alternative to the more conventional measurements of transmission and reflection and has the advantage, that only that part of the absorptivity leading to the generation of electron-hole pairs is determined, even if significant free-carrier absorption is present. © 1998 Elsevier Science B.V. All rights reserved.

*Keywords:* Absorptivity; Luminescence; Silicon solar cells

---

## 1. Introduction

The absorptivity  $A_{\text{BB}}(h\omega)$  for band-to-band transitions is a crucial quantity for the efficiency of a solar cell to which only those absorption processes generating an electron-hole pair contribute. In conventional absorption experiments other absorption processes like free-carrier absorption, which do not affect the density of electrons and holes, prevent the exact determination of  $A_{\text{BB}}(h\omega)$ . In such experiments, it is always the overall absorptivity which is measured.  $A_{\text{BB}}(h\omega)$  can be determined from the short-circuit-current response of a solar cell [1]. This requires the

---

\* Corresponding author. E-mail: peter.wuerfel@physik.uni-karlsruhe.de

pn-structure of a solar cell. While our results have been obtained from the electroluminescence of a solar cell photoluminescence from a homogenous material would work as well too.

Already in 1860 Kirchoff realized that the emission and the absorption of a body are closely related to each other [2]. He found that the ability of a body to emit light in a certain energy-interval is equal to its absorptivity  $A(\hbar\omega, T)$  in the same energy interval. He restricted himself to the emission and absorption of thermal radiation. Together with Planck's law, which describes the emission of a black body, the intensity of thermally emitted radiation of a non-black body is:

$$I_{\text{nonbb}}(\hbar\omega, T) = A(\hbar\omega, T) \cdot I_{\text{bb}}(\hbar\omega, T), \quad (1)$$

where  $I_{\text{nonbb}}(\hbar\omega, T)$  and  $I_{\text{bb}}(\hbar\omega, T)$  are the intensities emitted by a non-black body and a black body, respectively.

This equation allows to calculate the absorptivity  $A(\hbar\omega, T)$  of a body by simply dividing its thermally emitted spectrum by the spectrum which would be emitted by a black body of the same temperature and which is given by Planck's law.

In the case of luminescence spectra we deal with non-thermal radiation, to which Planck's law is not applicable. A generalization of Planck's emission law [3,4], however, describes photon emission by luminescence via direct or indirect transitions, by introducing a non-zero chemical potential  $\mu_\gamma$  for the emitted photons, which distinguishes luminescence from thermal radiation, for which  $\mu_\gamma = 0$ . This generalization is valid for optical transitions occurring between two sets of states, each of which is occupied according to a separate Fermi-distribution.

The validity of this generalized Planck's law has been proven experimentally for direct [5] and indirect [6] transitions in semiconductors. According to Refs. [3,4], the rate of spontaneous emission  $dr_{\text{em}}$  of photons with energy between  $\hbar\omega$  and  $\hbar\omega + d\hbar\omega$  into the solid angle  $\Omega$  is given by the absorption coefficient  $\alpha(\hbar\omega)$  at exactly this photon energy and by the chemical potential  $\mu_\gamma$ :

$$dr_{\text{em}}(\hbar\omega) = \alpha(\hbar\omega) \cdot \frac{c_\gamma D_\gamma \Omega}{\exp\left(\frac{\hbar\omega - \mu_\gamma}{kT}\right) - 1} d(\hbar\omega). \quad (2)$$

$c_\gamma = c_0/n$  is the velocity of the photons in the emitting medium with refractive index  $n$ , and  $D_\gamma = (n^3(\hbar\omega)^2)/(4\pi^3\hbar^3 c_0^3)$  is the density of states per solid angle for photons in the medium.

The chemical potential  $\mu_\gamma$  of the emitted photons is equal to the difference  $\varepsilon_{\text{F,C}} - \varepsilon_{\text{F,V}}$  of the quasi-Fermi energies, which describe separately the occupation of states in the conduction and valence bands, respectively. In thermal and chemical equilibrium with the surrounding blackbody radiation of 300 K,  $\varepsilon_{\text{F,C}} - \varepsilon_{\text{F,V}} = \mu_\gamma = 0$  and Eq. (2) reduces to the original Planck's law for thermal radiation.

If we consider the electroluminescence of a solar cell, the difference of the quasi-Fermi energies at the location of photon emission ideally equals the voltage at its terminals if voltage drops across series resistances can be neglected. For the emission

of electroluminescence at room temperature we have applied voltages between 0.7 and 0.8 V in the forward direction.

Because the energy of emitted photons is restricted to a small energy interval near the band gap ( $E_{\text{gap,Si}}(300 \text{ K}) \simeq 1.12 \text{ eV}$ ) the term  $-1$  in the denominator of Eq. (2) can be neglected so that this can be rewritten:

$$dr_{\text{em}}(\hbar\omega) = \alpha(\hbar\omega) \cdot c_{\gamma} D_{\gamma} \Omega \exp\left(\frac{-\hbar\omega}{kT}\right) \exp\left(\frac{\varepsilon_{\text{F,C}} - \varepsilon_{\text{F,V}}}{kT}\right) \cdot d(\hbar\omega). \quad (3)$$

In the following, we show how the generalized Planck's law can be used to extract the absorptivity of a solar cell from its emitted luminescence spectrum.

## 2. Theory

For the application of Eqs. (2) and (3), one has to distinguish between different absorption processes. The most important contributions to the total absorption coefficient  $\alpha(\hbar\omega)$  are band-to-band transitions and free-carrier absorption, which is an intraband transition.

$$\alpha(\hbar\omega) = \alpha_{\text{fc}}(\hbar\omega) + \alpha_{\text{bb}}(\hbar\omega). \quad (4)$$

Both absorption processes have their counterpart in emission processes.

In Fig. 1 experimental data for  $\alpha_{\text{bb}}(\hbar\omega)$ , the absorption coefficient for band to band transitions from Ref. [7], and calculated values for  $\alpha_{\text{fc}}(\hbar\omega)$ , the absorption coefficient for free-carrier absorption [8], are plotted as a function of the photon energy  $\hbar\omega$  for  $T = 300 \text{ K}$  and for a free-carrier density of  $10^{18} \text{ cm}^{-3}$ . The calculations for  $\alpha_{\text{fc}}(\hbar\omega)$  have been performed for p-type silicon.

For energies well below the band gap  $\alpha_{\text{fc}}(\hbar\omega)$  is up to  $10^8$  times larger than  $\alpha_{\text{bb}}(\hbar\omega)$ , while for energies  $\hbar\omega > E_{\text{gap}}$   $\alpha_{\text{bb}}(\hbar\omega)$  is dominant.

The contribution of free-carrier intraband transitions and of band–band transitions to the spontaneous emission rate is, however, not in proportion to the respective absorption coefficients.

One very important point in the derivation of the generalized Planck's law is the fact that transitions occur between two different energy ranges (the conduction band and the valence band) which are separated by an energy gap and which are separately described by two different Fermi distributions for the same temperature. This is not the case for free-carrier absorption, where transitions take place between states in the same Fermi distribution. The inverse process, the emission of a photon, when an electron makes a transition from a high- to a low-energy state within the Fermi distribution of the conduction band, is therefore purely thermal.

As a consequence, the factor  $\exp(\varepsilon_{\text{F,C}} - \varepsilon_{\text{F,V}})/kT$  only concerns  $\alpha_{\text{bb}}(\hbar\omega)$ :

$$dr_{\text{em}}(\hbar\omega) = \left[ \alpha_{\text{fc}}(\hbar\omega) + \exp\left(\frac{\varepsilon_{\text{F,C}} - \varepsilon_{\text{F,V}}}{kT}\right) \cdot \alpha_{\text{bb}}(\hbar\omega) \right] c_{\gamma} D_{\gamma} \Omega \exp\left(\frac{-\hbar\omega}{kT}\right) \quad (5)$$

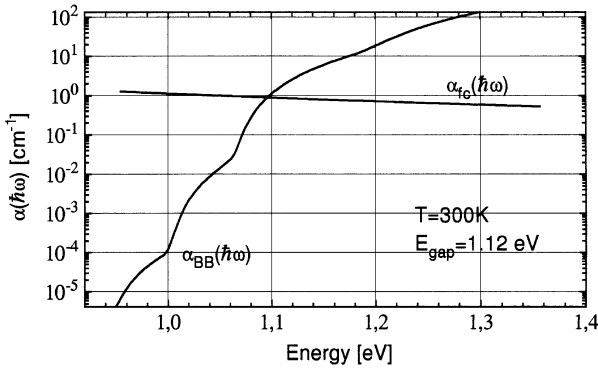


Fig. 1. Absorption coefficient  $\alpha_{fc}(h\omega)$  for free carrier absorption and  $\alpha_{BB}(h\omega)$  for absorption via band-to-band transitions.

For an assumed difference of the quasi-Fermi energies of 0.7 eV at  $T = 300$  K the factor  $\exp(\varepsilon_{F,C} - \varepsilon_{F,V})/kT$  is larger than  $10^{12}$ . Therefore, the spontaneous emission rate is solely determined by  $\alpha_{bb}(h\omega)$  and the emission of photons from electronic transitions within one band is completely negligible. Consequently,  $\alpha(h\omega)$  in Eq. (2) has to be replaced by  $\alpha_{bb}(h\omega)$ .

As an example, we will now consider a plan-parallel slab and calculate the emitted spectral energy current density  $j_E(h\omega)$  into the solid angle  $\Omega$  in the direction perpendicular to the surface.

The integration of the spontaneous emission rate from Eq. (2) over the thickness  $d$  of the slab yields:

$$\begin{aligned}
 dj_E(h\omega) = & CM(h\omega)\alpha_{bb}(h\omega)\exp[-\alpha(h\omega)d] \cdot (h\omega)^3 d\Omega d(h\omega) \\
 & \times \int_0^d \frac{\exp[\alpha(h\omega)z] + R_2(h\omega)\exp[-\alpha(h\omega)z]}{\exp\left[\frac{h\omega - (\varepsilon_{F,C}(z) - \varepsilon_{F,V}(z))}{kT}\right] - 1} dz
 \end{aligned} \tag{6}$$

with

$$M(h\omega) = \frac{1 - R_1(h\omega)}{1 - R_1(h\omega)R_2(h\omega)\exp[-\alpha(h\omega)d]}, \tag{7}$$

taking into account reabsorption and multiple reflections.  $C$  is a factor of proportionality.

To be able to calculate the spectral energy current density one has to know the spatial distribution of the difference of the quasi-Fermi energies. The diffusion length of the charge carriers in the investigated silicon solar cells is known to be much larger than the thickness of the cells. As a consequence, the distribution of electrons and holes apart from the very thin n-doped emitter of the cell is homogeneous and the difference of the quasi-Fermi-energies is constant. In this special case, the integral in

Eq. (6) can easily be solved, which yields

$$dj_E(\hbar\omega) = C \frac{\alpha_{bb}(\hbar\omega)}{\alpha(\hbar\omega)} A(\hbar\omega) \frac{(\hbar\omega)^3}{\exp\left[\frac{\hbar\omega - (\varepsilon_{F,C} - \varepsilon_{F,V})}{kT}\right] - 1} d(\hbar\omega), \quad (8)$$

where the absorptivity  $A(\hbar\omega)$  is related to the total absorption coefficient  $\alpha(\hbar\omega)$  in Eq. (4) by

$$A(\hbar\omega) = \frac{(1 - R_1)(1 - \exp[-\alpha d])(1 + R_2 \exp[-\alpha d])}{1 - R_1 R_2 \exp[-2\alpha d]}. \quad (9)$$

$R_1$  and  $R_2$  are the reflectivities of the front and the back surfaces, respectively, which depend on the photon energy ( $\hbar\omega$ ). Calculated values for  $\alpha_{bb}(\hbar\omega)/\alpha(\hbar\omega) \cdot A(\hbar\omega)$  for different free-carrier densities are shown in Fig. 2. As the investigated solar cells are made from p-type silicon, in the following free-carrier densities correspond to hole densities.

The curves for  $N_{fc} = 0$  and  $N_{fc} = 2 \times 10^{17} \text{ cm}^{-3}$  are identical. This shows that for free carrier densities smaller than  $2 \times 10^{17} \text{ cm}^{-3}$  the influence of  $\alpha_{fc}(\hbar\omega)$  on  $\alpha_{bb}(\hbar\omega)/\alpha(\hbar\omega) \cdot A(\hbar\omega)$  is negligible, and  $\alpha_{bb}(\hbar\omega)/\alpha(\hbar\omega) \cdot A(\hbar\omega)$  can be replaced by  $A_{BB}(\hbar\omega)$  in Eq. (8):

$$dj_E(\hbar\omega) = C A_{BB}(\hbar\omega) \frac{(\hbar\omega)^3}{\exp\left[\frac{\hbar\omega - (\varepsilon_{F,C} - \varepsilon_{F,V})}{kT}\right] - 1} d(\hbar\omega). \quad (10)$$

The investigated solar cells have resistivities between 0.5 and 10  $\Omega \text{ cm}$ , which corresponds to doping concentrations which are at least one order of magnitude below

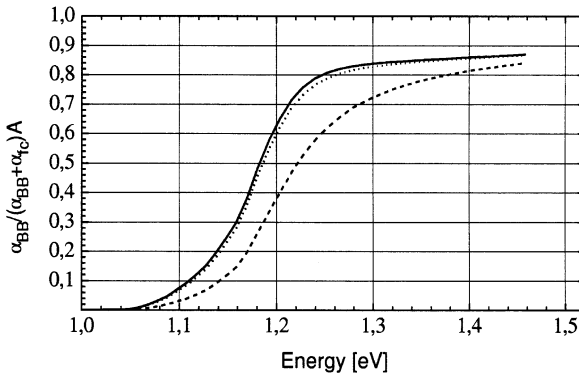


Fig. 2.  $\alpha_{BB}(\hbar\omega)/\alpha(\hbar\omega) \cdot A(\hbar\omega)$  for  $T = 300 \text{ K}$  and for different free-carrier densities,  $N_{fc} = 2 \times 10^{17} \text{ cm}^{-3}$  (solid line),  $10^{18} \text{ cm}^{-3}$  (dotted line) and  $10^{19} \text{ cm}^{-3}$  (dashed line), where  $A(\hbar\omega)$  is the absorptivity. The curves for  $N_{fc} = 0$  and  $N_{fc} \leq 2 \times 10^{17} \text{ cm}^{-3}$  are identical.

$2 \times 10^{17} \text{ cm}^{-3}$ . This justifies the above simplification for the investigation of these cells.

At room-temperature

$$\exp\left(\frac{\hbar\omega - (\varepsilon_{F,C} - \varepsilon_{F,V})}{kT}\right)$$

can be assumed to be much larger than unity because  $\hbar\omega \approx E_{\text{gap}}$ , which yields

$$dj_E(\hbar\omega) = C \exp\left(\frac{\varepsilon_{F,C} - \varepsilon_{F,V}}{kT}\right) A_{\text{BB}}(\hbar\omega)(\hbar\omega)^3 \exp\left(-\frac{\hbar\omega}{kT}\right) d(\hbar\omega). \quad (11)$$

This equation allows to calculate the absorptivity for band-to-band transitions from absolute values of the spectral energy current density. In this work we have measured relative intensities. This implies that only relative values for  $A_{\text{BB}}(\hbar\omega)$  can be derived from the measured spectra, which have to be converted to absolute values. As the absorptivity reaches the value  $1 - R_1(\hbar\omega)$  at high energies the conversion of relative values into absolute values is very simple, if the reflectivity  $R_1(\hbar\omega)$  of the front surface is known.

While  $R_1(\hbar\omega)$  of a polished,  $\text{SiO}_2$ -covered surface is easily calculated, the calculation of the same quantity for a textured surface requires a precise analysis of the structure.

Silicon solar cells with different surface geometries, namely polished on both sides and textured with inverted pyramids, have been investigated in this work. The above calculations have been performed for the simple case of a plan-parallel slab. Although the calculation of  $A_{\text{BB}}(\hbar\omega)$  is not possible for more complicated geometries, like the inverted pyramids, Eq. (11) remains valid for the connection of the absorption and the emission of textured solar cells, as long as electrons and holes are distributed homogeneously in the solar cell.

### 3. Experiments

The above considerations have been applied to our experimental investigations of the electroluminescence of silicon solar cells. The applied voltage was modulated sinusoidally at a frequency of 565 Hz. The emitted radiation was passed through a  $\frac{1}{4}$  m monochromator with a grating blazed at 1000 nm. We used a liquid- $N_2$ -cooled Ge-diode as detector and the transmittance of the whole setup was calibrated against the spectrum of a black-body radiator. The detector signal was observed by a current-voltage converter and a lock-in amplifier.

The investigated silicon solar cells have resistivities between 0.5 and 10  $\Omega \text{ cm}$  and a thickness of 270  $\mu\text{m}$ . The width of the inverted pyramids on the textured solar cells is about 10  $\mu\text{m}$  and these cells have a surface area of 2  $\text{cm} \times 2 \text{ cm}$ .

The temperature of the solar cell was measured with a thermocouple mounted on the front surface. Due to Joule heating the temperature of the cells was higher than room temperature.

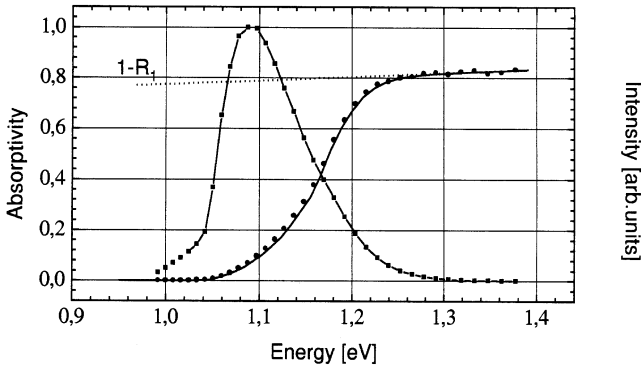


Fig. 3. Electroluminescence spectrum of the solar cell polished on both sides at  $T = 315$  K (solid line with squares), absorptivity  $A_{BB}(h\omega)$  extracted from this spectrum (full circles) and absorptivity  $A_{BB}(h\omega)$  calculated with literature data for  $\alpha_{BB}(h\omega)$  (solid line).

Fig. 3 shows the spectrum of a solar cell polished on both sides at  $T = 315$  K (squares). Relative values of the absorptivity  $A_{BB}(h\omega)$  were obtained by dividing the measured spectral energy current density by  $(h\omega)^3 \cdot \exp[-(h\omega)/kT]$  according to Eq. (11). In Fig. 3 relative values of  $A_{BB}(h\omega)$  (circles) have been adjusted to  $1 - R_1(h\omega)$  (dotted line) in the range of high photon energies.  $R_1(h\omega)$  is the calculated reflectivity of the front surface, which is covered with a 95 nm thick  $\text{SiO}_2$ -antireflection coating. The thickness of the  $\text{SiO}_2$ -layer was determined from measurements of the reflectivity of the cells at high energies, where back surface reflection is negligible.

The absorptivity for the plan-parallel geometry has also been calculated from Eq. (9) using literature data [1] for  $\alpha_{BB}(h\omega)$  obtained from the spectral response of the short-circuit current of silicon solar cells. As these measurements had been performed at  $T = 300$  K we have slightly corrected the data with regard to the temperature dependence of the band gap and the occupation probability of the TO-phonon. We find very good agreement between our experimental values for  $A_{BB}(h\omega)$  and the values calculated with literature data (solid line in Fig. 3). In the calculations we have assumed an energy-independent reflectivity of the back surface of  $R_2 = 0.81$ . This value has been confirmed from the measurements of the reflectivity at low energies, where the photons have a large penetration depth.

Texturing the front surface of solar cells has two reasons. The front surface reflectivity shall be reduced and the average path length within the cell shall be extended. Compared to a solar cell polished on both sides the absorptivity of a textured solar cell is expected to be substantially improved at lower photon energies. An analytical calculation of the absorptivity is not possible in this case.

An expression for the front surface reflectivity of the inverted pyramid structure for normal incidence is derived from geometrical optics:

$$R_{pyr}(h\omega) = 0.16 \cdot R_{\theta=0^\circ} + 0.5 \cdot R_{\theta=54.8^\circ} R_{\theta=15.6^\circ} + 0.34 \cdot R_{\theta=54.8^\circ} R_{\theta=78.9^\circ} R_{\theta=33.5^\circ}, \tag{12}$$

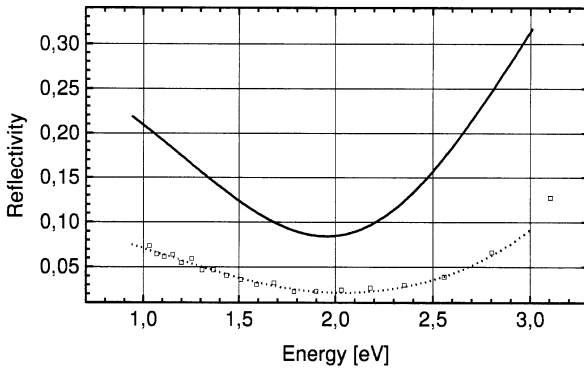


Fig. 4. Front surface reflectivity for normal incidence on a 105 nm antireflection coating (solid line) and for the inverted pyramid structure according to Eq. (12) (broken line). Squares correspond to the results of the ray-tracing simulation.

where  $R_{\theta=X}$  is the reflectivity of a single face for light which is incident under the angle  $\theta = X$  with respect to the face normal.

This expression has been obtained by an analysis of the investigated structure. It takes into account, that the so-called ridge tops make up about 16% of the surface area, while about 50% of the light undergo a double reflection and 34% undergo a triple reflection on the different faces of the inverted pyramids before being reflected away from the surface. This result could be verified by a ray-tracing analysis performed with the ray-tracing program SUNRAYS [9] (Fig. 4).

There is good agreement between the calculation and the simulation. The reduced reflectivity of the structured surface in comparison with the reflectivity  $R_{\theta=0^\circ}$  of the polished surface is clearly visible.

The absorptivity of the textured solar cell at  $T = 25^\circ\text{C}$  is shown in Fig. 5 in comparison with the absorptivity for planar polished surfaces according to Eq. (9). Again the relative values have been converted into absolute values by adjusting the high-energy absorptivity to  $(1 - R_{\text{pyr}}(\hbar\omega))$ . The effect of a 105 nm  $\text{SiO}_2$  antireflection-coating is taken into account in our calculations.

The average path length of weakly absorbed light within the textured solar cell is enhanced compared to the average path length within a cell with polished surfaces, which results in an enhanced absorptivity for weakly absorbed photons.

Theoretical calculations [10,11] yield an average path length enhancement of  $4n^2$  for very weakly absorbed photons for a cell with a perfectly reflecting back surface and a totally randomizing (Lambertian) front surface, where  $n$  is the refractive index of the solar cell material. For silicon this factor equals  $4n^2 = 46$ .

Under the condition of weak absorption the absorptivity of such a cell can be calculated approximately [12]:

$$A = \frac{1 - R(\hbar\omega)}{\frac{1 - R(\hbar\omega)}{4n^2\alpha(\hbar\omega)d} + 1} \quad (13)$$

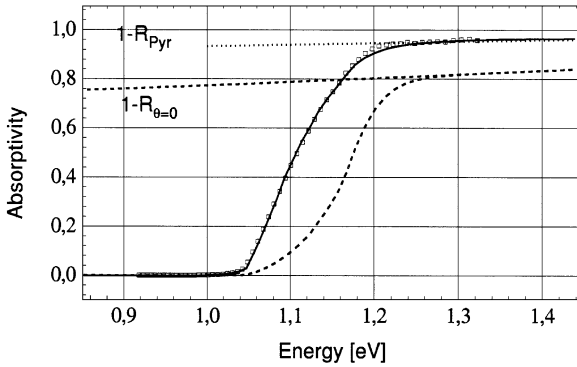


Fig. 5. Absorptivities  $A_{BB}(\hbar\omega)$  of the solar cell textured with inverted pyramids (squares) and of the solar cell polished on both sides for  $T = 315$  K (broken line) and  $A_{BB}(\hbar\omega)$  calculated from Eq. (14) (solid line).

where  $R(\hbar\omega)$  is the reflectivity of the front surface and the term  $4n^2$  describes the enhanced average path length.

According to ray-tracing calculations in Ref. [13], the path length enhancement of a solar cell with inverted pyramids on the front surface varies with the thickness of the cell and takes on values between 12 and 43, where the maximum value is achieved, when an optimum condition for the thickness of the cell is fulfilled.

In the low-energy region of weak absorption the absorptivity of the textured solar cell obtained from the emitted luminescence spectrum, can be described by Eq. (13) if the term  $4n^2$  is replaced by the value 16, which implies that the average path length is only enhanced by a factor of 16 (Fig. 5):

$$A = \frac{1 - R(\hbar\omega)}{\frac{1 - R(\hbar\omega)}{16\alpha(\hbar\omega)d} + 1} \tag{14}$$

The factor 16 being close to the lower limit for the path length enhancement indicates that the optimum condition for the thickness of the cell in [13] is not fulfilled. The back surface reflection of 0.81 is one more reason for this low value.

According to [13] the variation of the path length enhancement with the thickness of the cell has a simple geometrical explanation. In an inverted pyramid the face through which a photon is coupled into the cell has two adjacent faces and one opposite face. Rays which, after reflection on the back surface, restrike the front surface on a face parallel to the opposite face, lie inside the escape cone and leave the cell.

On the contrary a ray which strikes a face parallel to one of the adjacent faces is totally reflected and remains trapped. The fraction of light striking the front surface on a face parallel to the opposite or an adjacent face depends on the thickness of the cell, which leads to the above mentioned variation of the average path length.

In much the same way, the average path length and as a result also the absorptivity of the cell depend on the angle of incidence of light. This has been affirmed by

a ray-tracing analysis of the angular dependence of the collection efficiency of textured silicon solar cells by Smith [14].

Following our method of relating the emission to the absorptivity of the cell the variation of the path length enhancement with the angle of incidence should show up in the angular dependence of the emitted luminescence intensity. The so-called “hot spots” with very high collection efficiency, mentioned in Ref. [14], should correspond to angles, under which the emitted luminescence intensity is increased.

The angular dependence of the emitted intensity was measured by moving the cell in 3 mm steps over an area of  $240 \text{ mm} \times 240 \text{ mm}$  in a distance of 780 mm of the fixed detector (Fig. 6). Besides the cosine angular dependence, which is due to the fact that only the projection of the cell is visible by the detector, a distinct structure of minima and maxima appears. The distance between two maxima in Fig. 7 corresponds to an angle of  $2.95^\circ$ .

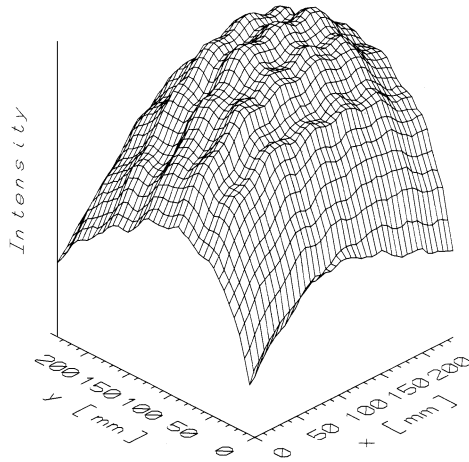


Fig. 6. Angular dependence of the emitted intensity of the textured solar cell. The distance between two maxima corresponds to an angle of  $2.95^\circ$ .

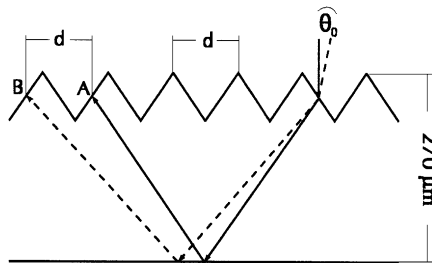


Fig. 7. Two-rays incident normally and under the angle  $\theta_0$  to the front surface restrike the front surface after reflection at the back surface at point A and point B, which are separated by the width of one inverted pyramid.

This structure could definitely be assigned to the above mentioned angular dependence of the path length enhancement.

In Fig. 7 two rays incident under different angles on the same face of an inverted pyramid are compared. One of them is incident normally to the surface of the cell and assuming low absorption, this ray is reflected at the back surface of the cell and restrikes the front surface in point A.

We calculated the angle  $\theta_0$  under which the other ray has to be incident in order to restrike the front surface shifted exactly by the width of one pyramid in point B (Fig. 7). Restriking the front surface shifted by one pyramid means that the fraction of light striking an opposite face and an adjacent face, respectively, are the same for the ray incident normally and the ray incident under the angle  $\theta_0$ . This results in the same average path length and the same absorptivity for these two rays. For a thickness of 270  $\mu\text{m}$  and a width of the pyramids of  $d = 10 \mu\text{m}$  this calculation yields  $\theta_0 = 2.97^\circ$ , which agrees well with the experimental value.

The spectral analysis of the angular dependence of the luminescence intensity confirms this explanation. The structure in the angular distribution is not observable at wavelengths shorter than 1050 nm, because light with shorter wavelengths is absorbed before it restrikes the front surface.

#### 4. Conclusion

The absorptivity for band-to-band transitions of silicon solar cells can be extracted from their luminescence spectra for a planparallel geometry as well as for textured surfaces where transmission and reflection measurements are difficult due to light scattering by the surface texture and must be performed in an Ulbricht-sphere. Deducing the absorptivity for band-band transitions is uncertain because of the unknown absorption in the metallic back contact. With our method, the absorptivity for band-band transitions can be determined even in a spectral range, where it is completely masked by free carrier absorption which may be orders of magnitude larger than the absorption via band-to-band transitions. In this case it is not accessible by transmission and reflection measurements. The method we have presented is applicable to solar cells with all kinds of textured surfaces and is not restricted to silicon solar cells.

#### Acknowledgements

We are grateful to Dr. Warta, ISE, Freiburg, Germany for providing the textured silicon solar cells and to Dr. K. Widder from our institute for measuring their reflectivities.

#### References

- [1] M.J. Keevers, M.A. Green, *Appl. Phys. Lett.* 66 (2) (1995) 174–176.
- [2] G. Kirchhoff, *Ann. Physik* 19 (1860) 275–301.

- [3] P. Würfel, *J. Phys. C* 15 (1982) 3967.
- [4] P. Würfel, S. Finkbeiner, E. Daub, *Appl. Phys. A* 60 (1995) 67–70.
- [5] B. Feuerbacher, P. Würfel, *J. Phys. C* 2 (1990) 3803–3810.
- [6] K. Schick, E. Daub, S. Finkbeiner, P. Würfel, *Appl. Phys. A* 54 (1992) 109.
- [7] E. Daub, P. Würfel, *Phys. Rev. Lett.* 74 (6) (1995) 1020–1023.
- [8] P.E. Schmidt, *Phys. Rev. B* 23 (10) (1981) 5531–5536.
- [9] R. Brendel, 12th European Photovoltaic Solar Energy Conf. Amsterdam, April 1994.
- [10] E. Yablonovitch, G.D. Cody, *IEEE Trans. Electron Dev.* ED-29 (1982) 300–305.
- [11] E. Yablonovitch, *J. Am. Soc.* 72 (1982) 899.
- [12] P. Würfel, *Physik der Solarzellen*, Spektrum Akademischer Verlag GmbH, Heidelberg, Berlin, Oxford, 1995.
- [13] P. Campbell, M.A. Green, *J. Appl. Phys.* 62 (1) (1 July 1987) 243–249.
- [14] A.W. Smith, *Sol. Energy Mater. Sol. Cells* 32 (1994) 37–51.